

# Effect of CdS modification on photoelectric properties of TiO<sub>2</sub>/PbS quantum dots bulk heterojunction

Xin Shi<sup>a,b</sup>, Jianping Xu<sup>b,\*</sup>, Shaobo Shi<sup>c</sup>, Xiaosong Zhang<sup>b</sup>, Shubin Li<sup>b</sup>, Chang Wang<sup>b</sup>, Xueliang Wang<sup>b</sup>, Linlin Li<sup>b</sup>, Lan Li<sup>b,\*</sup>

<sup>a</sup> College of Science, Tianjin University of Technology, Tianjin 300384, China

<sup>b</sup> Institute of Material Physics, Key Laboratory of Display Materials and Photoelectric Devices, Ministry of Education, Tianjin University of Technology, Tianjin 300384, China

<sup>c</sup> School of Science, Tianjin University of Technology and Education, Tianjin 300222, China

## ARTICLE INFO

### Article history:

Received 27 November 2015

Received in revised form

2 January 2016

Accepted 20 January 2016

Available online 21 January 2016

### Keywords:

Quantum dots

Bulk heterojunction

Defect states

Trap states

## ABSTRACT

TiO<sub>2</sub>/PbS(CdS) quantum dots (QDs) bulk heterojunction has been fabricated by successive ionic layer adsorption and reaction method via alternate deposition of PbS and CdS QDs. In comparison with TiO<sub>2</sub>/PbS heterojunction, the incident photon to current conversion efficiency was increased almost 50% in the visible region. Meantime, the short-circuit current and open-circuit voltage were enhanced 200% and 35% respectively. The influence mechanism of CdS is related to reduction of trap state density at TiO<sub>2</sub>/PbS interface and PbS QDs surface by the discussion of the dark current density–voltage curves, the transient photocurrent response curves and the electrochemical impedance spectra spectroscopy (EIS).

© 2016 Published by Elsevier Ltd.

## 1. Introduction

Semiconductor quantum dots (QDs) based bulk heterojunction (i.e. three-dimension) structure, in which n- or p-type QDs intimately interpenetrated or interconnected, is regarded as an effective route for improving the performance of photoelectric devices such as photovoltaic devices [1,2], light-emitting devices [3,4], photocatalytic [5,6] and photodetectors [7,8]. Rath et al. [9] reported that the conversion efficiency of hybrid Bi<sub>2</sub>S<sub>3</sub>/PbS QDs bulk heterojunction solar cell was threefold higher than planar heterojunction devices. The hybrid structure can enlarge the heterojunction area and then allow rapid charge-carrier separation at the interface [10,11]. The QDs based bulk heterojunction films are generally fabricated from ex situ [12] and in situ chemical methods [13]. The in situ method such as successive ionic layer adsorption and reaction (SILAR) can form continuous and dense thin films with controlled thickness using a simple equipment under mild reaction conditions, which can produce a good interface contact between QDs and function layer and realize the attachments of QDs into the array and mesoporous structures to form the bulk heterojunctions [14]. Nanostructured interfaces will enable improved charge separation and electron extraction by allowing a

greater volume of light-absorbing QDs film to be incorporated into a device. On the other hand, the SILAR method can avoid introducing long-chain organic ligands, such as oleic acid, which are used in the synthesis of QDs by hot injection method and can create a large barrier to electronic transport. By direct growth of nanoparticles inside the mesoporous film or nano-arrays, the bulk heterojunction structure can be got a better interlaminar contact [15].

N-type TiO<sub>2</sub> attracted numerous research interests for its catalytic and energy-related applications due to its appropriate electronic band structure and excellent surface activity [16]. Nevertheless, its relatively poor charge transport property and wide band-gap are main limitations for the applications. The narrow band-gap sensitizer such as CdSe, CdTe and PbS QDs can widen absorption spectra, enhance absorption and improve charge-separation efficiency [17]. The interface/surface defects, considered as carrier recombination centers and inhibit the carrier transport and collection [18], can be passivated by inorganic materials [19]. Kemp et al. [20] reported that the optimization of ZnO layer on the surface of PbS QDs can reduce TiO<sub>2</sub>/PbS QDs interface recombination and improve the interface contact. Guijarro et al. [21] found ZnS deposition layer on CdSe QDs thin film can enhance a PCE (photoelectric conversion efficiency) of the solar cell. The reduction of surface defects of CdSe QDs films induces the decrease of carrier recombination at CdSe QDs/electrolyte interface.

\* Corresponding authors.

E-mail addresses: [xjp0335@163.com](mailto:xjp0335@163.com) (J. Xu), [lilan@tjut.edu.cn](mailto:lilan@tjut.edu.cn) (L. Li).

Although defects passivation can improve threefold PCE for PbS@CdS core-shell QDs based solar cell [22], the organic molecules were inevitably introduced into PbS@CdS QDs via hot colloidal solution chemistry. It is important process to passivate the surface defects of QDs without generating other organic molecules.

In the report, the all-inorganic  $\text{TiO}_2/\text{PbS}$  QDs bulk heterojunction and  $\text{TiO}_2/\text{PbS}(\text{CdS})$  bulk heterojunction were fabricated. The in situ alternating deposition of PbS and CdS QDs on the surface of  $\text{TiO}_2$  nanocrystal film was performed via SILAR at ambient conditions. The effects of CdS QDs on the trap state density, transient photocurrent response time and charge transport processes were discussed for  $\text{TiO}_2/\text{PbS}$  QDs heterojunction.

## 2. Experimental

Briefly, 10 ml titanium butoxide ( $\text{C}_{16}\text{H}_{36}\text{O}_4\text{Ti}$ ) and 1 ml acetic acid aqueous solution ( $\text{V/V}=1:1$ ) were dissolved in 53 ml and 27 ml high purity ethanol, respectively. Then, the acetylacetone was added to mixed solution and maintained for 6 h at  $30^\circ\text{C}$  with vigorous magnetic stirring. Finally, 0.9 ml N-N dimethyl formamide (DMF) was added to the resultant and then the  $\text{TiO}_2$  sol-gel solution can be obtained after stirring for 0.5 h. The fluorine-doped tin oxide (FTO) glass was cleaned sequentially by using liquid detergent, deionized water, acetone, isopropanol and ethanol under ultrasonic agitation. After that, as-prepared sol-gel solution was spin coated on FTO glass at 2500 rpm for 25 s, followed by the baking temperature at  $500^\circ\text{C}$  for 10 min. After repeated the procedure for 4 times, the  $\text{TiO}_2$  film was sintered at  $500^\circ\text{C}$  for 2 h to remove the residual solvent. Then, the PbS(CdS) QDs layer on  $\text{TiO}_2$  thin films were prepared by SILAR method. The FTO glass with grown  $\text{TiO}_2$  layer was thoroughly dipped into 0.02 M  $\text{Pb}(\text{CH}_3\text{COO})_2$  methanol solution and  $\text{Na}_2\text{S}$  methanol/water ( $\text{V/V}=1:1$ ) solution successively, both with 40 s, and then rinsed with methanol vigorously. After that, the CdS preparation process is similar to that of PbS by immersing as-prepared films in 0.05 M  $\text{Cd}(\text{CH}_3\text{COO})_2$  methanol solution and 0.05 M  $\text{Na}_2\text{S}$  methanol/water ( $\text{V/V}=1:1$ ) solution as cadmium and sulfur source for 20 s, respectively. The two processes were regard as one cycle. The alternate deposition of PbS and CdS layers, which was represented as PbS(CdS), is developed for cycles as high as 5. After deposition, the samples were annealed at  $200^\circ\text{C}$  for 1 h in nitrogen. Finally, an Au top electrode with thickness about 100 nm was deposited on as-prepared film by thermal evaporation under high vacuum of  $5 \times 10^{-4}$  Pa. The active area was defined to be  $0.04\text{ cm}^2$  using a shadow mask. For comparison, the reference sample without CdS was constructed using the similar procedure. The schematic illustrations for  $\text{TiO}_2/\text{PbS}$  QDs and  $\text{TiO}_2/\text{PbS}(\text{CdS})$  QDs bulk heterojunctions are shown in Fig. 1(a) and (b), respectively.

The crystal structures of heterojunctions were characterized by

using Rigaku 2500/PC X-ray diffractometer (XRD) with Cu K $\alpha$  radiation source (0.1542 nm) at 40 kV and 150 mA. Field emission scanning electron microscope (FESEM, JEOL JSM-71001F) was used to describe the morphology of the heterojunctions. The current-voltage ( $I$ - $V$ ) characteristics of the heterojunctions were surveyed with Keithley 2400 sourcemeter under dark and solar simulator illumination of  $100\text{ mW cm}^{-2}$  (AM 1.5 G). Incident photon to current conversion efficiency (IPCE) was analyzed under monochromatic light by a 300 W Xe lamp illuminating. The absorption spectra were recorded by UV-visible spectrophotometer (Hitachi U-4100, Japan). The transient photocurrent responses were determined with a Keithley 2400 sourcemeter under a 980 nm laser illumination. The electrochemical impedance spectra (EIS) were gauged over 100 kHz to 50 mHz by electrochemical workstation (CHI 660D, Chenhua Instruments, China) in mixture solution containing of 0.25 M  $\text{Na}_2\text{S}$  and 0.35 M  $\text{Na}_2\text{SO}_3$  at 0 V versus Ag/AgCl. All the measurements were carried out in ambient atmosphere.

## 3. Results and discussion

The XRD patterns of  $\text{TiO}_2/\text{PbS}$ ,  $\text{TiO}_2/\text{CdS}$  and  $\text{TiO}_2/\text{PbS}(\text{CdS})$  films are shown in Fig. 2. All the films exhibit strong diffraction peaks at  $2\theta=25.3^\circ$ ,  $37.8^\circ$  and  $48.0^\circ$ , corresponding to the (101), (004), and (200) planes of anatase  $\text{TiO}_2$ . The main intense diffraction peaks of  $\text{TiO}_2/\text{PbS}$  film at  $26.0^\circ$ ,  $30.1^\circ$ ,  $43.1^\circ$  and  $51.0^\circ$  are indexed as galena PbS (JCPDS no. 10-0454), indicating the PbS QDs was obtained. The mean crystallite size for PbS is calculated at about 10 nm by Scherrer equation. The broad weak diffraction peaks of  $\text{TiO}_2/\text{CdS}$  film at  $2\theta=26.5^\circ$ ,  $30.8^\circ$ , and  $43.9^\circ$  (marked with red circle) are correspond to hawleyite CdS (JCPDS no. 10-0454). The diffraction peaks of  $\text{TiO}_2/\text{PbS}(\text{CdS})$  film and  $\text{TiO}_2/\text{CdS}$  have small shift to high angle compared with that of  $\text{TiO}_2/\text{PbS}$  film. CdS can be formed by co-sharing an S atom situated in the face-centered cubic sublattice with PbS due to the small lattice mismatch [23]. Hossain et al. reported that the presence of CdS in PbS phase after annealing process [24]. From the standard XRD data of CdS and PbS, the peak locations of the two phases are similar and those of CdS have small shift to high angle. The XRD patterns of the three films indicate that the CdS and PbS coexist in the  $\text{TiO}_2/\text{PbS}(\text{CdS})$  film.

Fig. 3 displays the FESEM images for all as-grown films. The top-view and cross-sectional images of  $\text{TiO}_2$  nanocrystal film (see Fig. 3(a)) demonstrate the rough surface structure with uniform and random distribution pores. After PbS deposition, the film becomes compact and devoid of pores as shown in Fig. 3(b). By SILAR method, ionic state of  $\text{Pb}^{2+}$  and  $\text{S}^{2-}$  can easily infiltrate into the pores of  $\text{TiO}_2$  film and react to PbS products in the liquid environment. From the cross-sectional view of  $\text{TiO}_2/\text{PbS}$  and  $\text{TiO}_2/\text{PbS}(\text{CdS})$  films shown in Fig. 3(c) and (d), the thickness of the

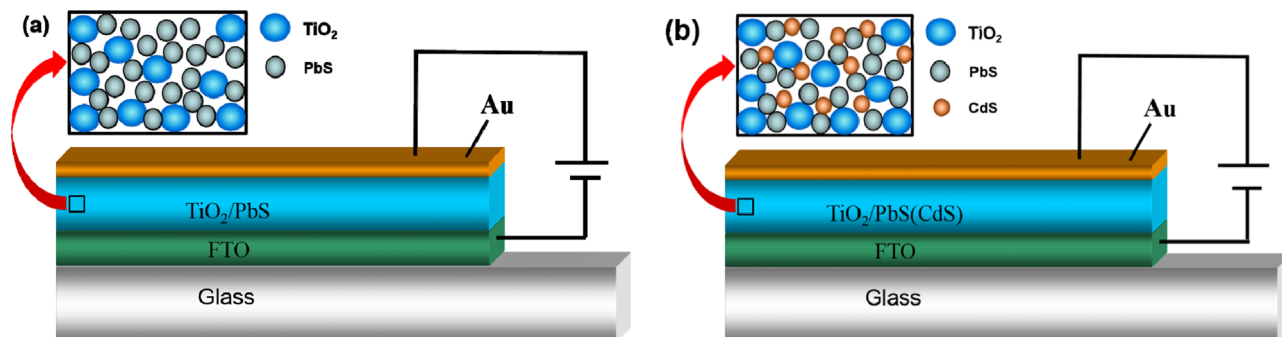


Fig. 1. The schematic diagrams for the heterojunction devices. (a)  $\text{TiO}_2/\text{PbS}/\text{Au}$  and (b)  $\text{TiO}_2/\text{PbS}(\text{CdS})/\text{Au}$ .

Download English Version:

<https://daneshyari.com/en/article/1515283>

Download Persian Version:

<https://daneshyari.com/article/1515283>

[Daneshyari.com](https://daneshyari.com)